Non-Trivial Lasing Mode From Parity-Time Symmetric Diffraction Gratings

Tahere Hemati and Binbin Weng*
School of Electrical and Computer Engineering, University of Oklahoma, Norman OK 73019
(Dated: July 22, 2021)

In this research, for the first time, active diffraction gratings as optical PT-symmetric platforms are studied. Through numerical and analytical studies, the bifurcation as the featured property in PT-symmetric systems is indicated. Moreover, it is shown that in addition to the gain/loss value, the period selection can push the system from the PT-symmetry to the symmetry-broken phase. Accomplished numerical simulations by the Rigorous Coupled-Wave Analysis (RCWA) method indicates the existence of Spectral Singularities (SSs) corresponding to single-mode, zero-bandwidth resonant peaks. The guiding procedure for fulfilling SSs in PT-symmetric diffraction gratings is related to the unique behavior of the scattering matrix in these kinds of gratings. The purpose of this study is to fill the research gap related to active PT-symmetric diffraction gratings and introducing new functionalities for these structures, including low-threshold and super-coherent lasers, which can advance the performance of on-chip optoelectronic devices.

I. INTRODUCTION

Diffraction gratings as the first optical components operating at subwavelength region can be considered the aspiration of modern nano-photonics concepts such as photonic crystals and metamaterials [1]. The main purpose of all these optical components is to control the light dynamic in a special way in nanometer-scale [2]. Today, the applications of diffraction gratings are expanded from telecommunications [3] and astronomy [4] to chemistry [5] and biosensing [6]. The recent progress in nano-fabrication technologies enabled us to create highly precise diffraction gratings and revealed the potential of these optical components in practice. Thus, in the recent decade, special attention has been attracted to this field.

The unique properties of diffraction gratings are associated with the spatial modulation of the Refractive Index (RI). Due to the diffraction, the amplitude and phase of the incident wave on a grating are modified. By optimizing grating parameters such as period, we can design the diffraction grating for different purposes, and the grating can operate as an optical filter [7], reflector [8], absorber [9], resonator [10], and go on.

More recently, by drawing the fundamental concepts in quantum physics such as Parity-Time (PT) symmetry to the realm of optics and photonics, novel applications, such as unidirectional emission [11] and asymmetric diffraction [12], appeared for periodical structures, including diffraction grating. The simplest definition of a PT-symmetric system is a non-Hermitian system whose Hamiltonian remains invariant under spatial reflection ($p \rightarrow -p$, $x \rightarrow -x$) and time-reversal ($p \rightarrow -p$, $x \rightarrow x$, $i \rightarrow -i$) operators, where p, x, and i are momentum, location, and imaginary unite, respectively [13]. It is indicated that to satisfy this condition the related potential should be $\hat{V}(x) = \hat{V}^*(-x)$. The equivalent condition for a optical system is $n(x) = n^*(-x)$ [14].

In practice, two identical coupled waveguides, one showing loss and the other one indicates the same amount of gain, can be the simplest example of an optical PT-symmetric system [14]. In this system, by increasing the gain/loss contrast between these two waveguides, the system transits from a PT-symmetric regime where all eigenvalues are real into a PT-broken regime where the eigenvalues are complex. There is a transient point between these two regimes named exceptional point, where both eigenvalues and eigenstates coalesce [15]. The uniqueness of a PT-symmetric system lies in indicating real eigenvalues, despite the non-Hermiticity and non-orthogonality of its eigenstates [16], which lead to extraordinary phenomena. Indeed, in PT-symmetric systems, we take advantage of the beneficial role of loss, while in trivial systems, loss always has a destructive effect, and it should be eliminated.

Scholars gradually found that using more complicated optical platforms such as periodical structures to realize the PT-symmetry concept can introduce new non-trivial outcomes, including loss-induced transparency [17], non-reciprocal light propagation [18], unidirectional invisibility [11, 19], and directional emission [20]. Among different kinds of periodical structures, only a few works have focused on diffraction gratings as a platform for indicating PT-symmetric effects [21, 22], and the accomplished works do not go beyond investigating asymmetric diffraction. Furthermore, to the best of our knowledge, no active PT-symmetric diffraction grating has been studied yet, and all the previous works investigated passive gratings. Therefore, it seems that there is a research gap in active PT-symmetric diffraction gratings and examining the possible new non-trivial phenomena besides asymmetric diffraction effect. This research will theoretically and numerically study the emission properties of diffracted modes from an active grating by Helmholtz equation, driving the related Hamilton and indicating symmetry and symmetry-broken and exceptional point regions. Moreover, the properties of resonating modes induced by PT-symmetric diffraction grating will be discussed in detail.

* binbinweng@ou.edu

II. THEORY AND ANALYTICAL SOLUTIONS

As we mentioned in introduction, the guiding procedure in diffraction gratings lies in spatial RI modulation. On the other hand, to realize PT-symmetry, RI modulation needs to satisfy $n(x) = n^*(-x)$. Therefore, the real part of RI modulation has to be a symmetric function and its imaginary part should be an asymmetric function. Thus the RI modulation can be defined as:

$$n(x) = n_0 + n\cos(2\pi x/a) + i\gamma\sin(2\pi x/a) \tag{1}$$

where a is the period, n_0 is the background refractive index, and n and γ are the real and imaginary parts of the refractive index modulation, respectively.

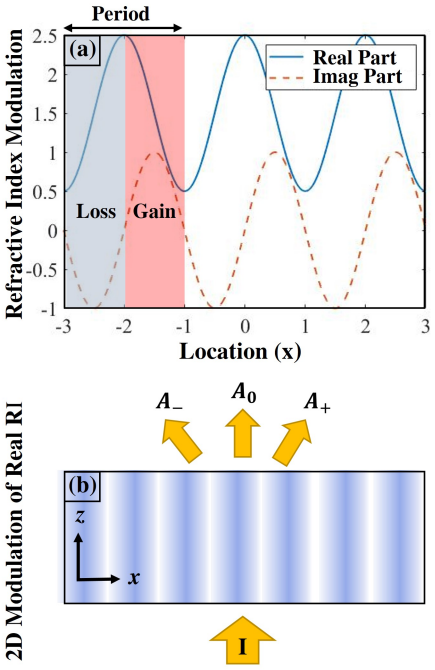

FIG. 1. (a) Real and imaginary parts of a PT-symmetric RI modulation in the x-direction .(b) Real RI modulation in x- and z-direction.

Figure 1.(a) shows the real (solid blue line) and imaginary (red dashed line) parts of the PT-symmetric refractive index distribution. The positive part of the imaginary RI indicates gain, and the negative part shows the induced loss. Figure 1.(b) displays the real part of RI modulation in two dimensions where the RI solely changes in the x-direction, and the incident light is perpendicular to the periodicity. A_-, A_0, and A_+ show the amplitude of the -1, 0, and $+1$ orders of diffracted modes, respectively.

In this research, we study the wave propagation of an incident light entering along the z-axis where the wave $E(x, z)$ obeys the Helmholtz equation [23, 24]:

$$\nabla^2 E + k_0^2 n^2(x) E = 0 \tag{2}$$

where $k_0 = 2\pi/\lambda$. Since, the incident light is normal to the periodicity both x and z components are effective. The general solution for $E(x, z)$ can be derived by Bloch's wave equation.

$$E(x, z) = u(x)e^{i\vec{\beta}.\vec{r}} \tag{3}$$

where $u(x)$ is a periodic function in the x-direction

$$u(x) = \sum_{m=-\infty}^{\infty} A_m e^{-i2\pi m x/a} \tag{4}$$

and in a 2D plane

$$e^{i\vec{\beta}.\vec{r}} = e^{i\beta_x x} e^{i\beta_z z} \tag{5}$$

By substituting equation 4 and 5 in equation 3:

$$E(x, z) = \sum_{m=-\infty}^{\infty} A_m e^{i\beta_z z} e^{i(\beta_x - 2\pi m/a)x} \tag{6}$$

To find β_x and β_z we should use the phase matching rule and dispersion relation. According to the phase matching:

$$\beta_x - 2\pi m/a = k_{x,inc} - 2\pi m/a \tag{7}$$

$$k_{x,inc} = k_0 n_{inc}\sin(\theta_{inc})$$

where $k_{x,inc}$, n_{inc}, and θ_{inc} are the wavenumber the refractive index and angle of the incident light, respectively. Since the incident angel is zero $k_{x,inc} = 0$, consequently $\beta_x = 0$. According to the dispersion relation, shown in equation 8.

$$\beta_z = \sqrt{k_0^2 n_0^2 - (2\pi m/a)^2} \tag{8}$$

If we consider the grating in diffracted regime where $a >> \lambda$, β_z will be reduced to $\beta_z = k_0 n_0$. Now by substituting β_z and β_x in equation 6:

$$E(x, z) = \sum_{m=-\infty}^{\infty} A_m e^{-i[mKx - k_0 n_0 z]} \tag{9}$$

where A_m is the amplitude of the m_{th} diffracted mode, and $K = 2\pi/a$.

To analytically solve equation 2, in addition to $E(x, z)$ we need to find $n^2(x)$ function. Through equation 1, supposing n and γ are significantly smaller than n_0, the squared of RI modulation can be rephrased as:

$$n^2(x) = n_0^2 + n_0[c^+ e^{iKx} + c^- e^{-iKx}] \tag{10}$$

where $c^+ = n + \gamma$ and $c^- = n - \gamma$. Now, by substituting equations 9 and 10 into equation 2, a set of coupled equations (equation 11) is obtained. It should be noted that to achieve equation 11, we only considered the first three orders (0, -1, and,+1 orders) [25].

$$\frac{\partial A_0}{\partial z} - \frac{ik_0}{2}[c^- A_1 + c^+ A_{-1}] = 0$$

$$\frac{\partial A_1}{\partial z} + \frac{iK^2 A_1}{2k_0 n_0} - \frac{ic^+ k_0 A_0}{2} = 0 \qquad (11)$$

$$\frac{\partial A_{-1}}{\partial z} + \frac{iK^2 A_{-1}}{2k_0 n_0} - \frac{ic^- k_0 A_0}{2} = 0$$

If we write equation 11 in a matrix form, the related Hamilton would be

$$H = \begin{bmatrix} \sigma & -k_0 c^+/2 & 0 \\ -k_0 c^-/2 & 0 & -k_0 c^+/2 \\ 0 & -k_0 c^-/2 & \sigma \end{bmatrix} \qquad (12)$$

where $\sigma = K^2/2k_0 n_0$. The eigenvalues of this Hamiltonian are:

$$\lambda_1 = \sigma$$

$$\lambda_2 = 1/2[\sigma - \sqrt{4k_0^2(n^2 - \gamma^2) + \sigma^2}] \qquad (13)$$

$$\lambda_3 = 1/2[\sigma + \sqrt{4k_0^2(n^2 - \gamma^2) + \sigma^2}]$$

While λ_1 is independent of real and imaginary refractive index modulation, λ_2 and λ_3 are dependent on the real and imaginary parts. Thus, once the condition 14 is satisfied, the system will be located at its exceptional point, and λ_2 and λ_3 and their related eigenstates coalesce.

$$\gamma = \sqrt{n^2 + \frac{\sigma^2}{4k_0^2}} \qquad (14)$$

Therefore, once the imaginary part of refractive index modulation is $\mid \gamma \mid > \sqrt{n^2 + \frac{\sigma^2}{4k_0^2}}$, the system enters into the symmetry-broken phase, indicating imaginary eigenvalues. Figures 2.(a) and 2.(b) show the real and imaginary part of eigenvalues according to the imaginary part of refractive index (γ), respectively, where dashed blue line indicates λ_2 and solid red line displays λ_3. As we can see, in the symmetry region, both eigenvalues show pure real value. However, immediately after the exceptional point, shown here by dashed gray line, two eigenvalues bifurcates so that one of them possesses a negative imaginary part (λ_3) and the other one indicates a positive imaginary part (λ_2). It can be interpreted that one mode is trapped mostly in gain and the other one captured in loss and suppressed. The bifurcation is the most remarkable property of PT-symmetric systems [26, 27]. This unique property is used in designing single-mode lasers [28, 29], where undesired competing modes are captured in the loss and suppressed, and only confined modes in the gain are amplified.

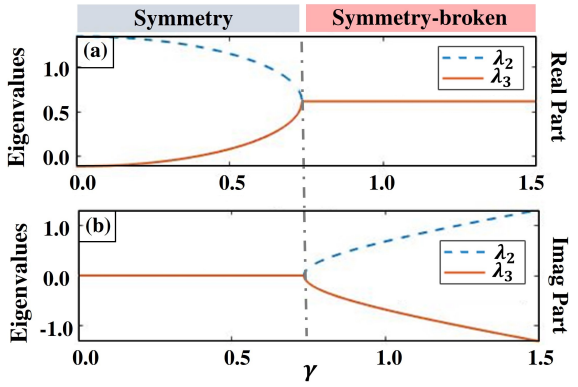

FIG. 2. (a) Real part and .(b) Imaginary part of eigenvalues according to the γ for a system with the periodicity of 2 μm. The exceptional point is shown by dashed gray line.

In gratings that incident light is parallel to the periodicity (along x-direction in figure 1.(b)), only the ratio between real and imaginary parts of refractive index (n and γ) determines the phase of the system [19]. However, in our designed grating, where the incident light is perpendicular to periodicity, the period plays an essential role.

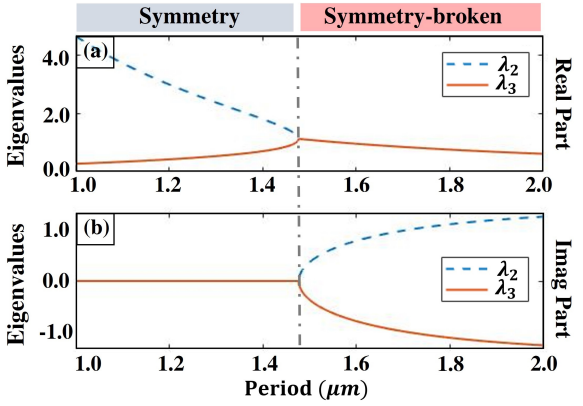

FIG. 3. (a) Real and .(b) Imaginary parts of eigenvalues according to the period for a PT-symmetric grating. The exceptional point is shown by dashed gray line.

Figure 3.(a) and 3.(b) show the real and imaginary part of eigenvalues shows the real and imaginary parts of eigenvalues according to different period selections, respectively. This figure demonstrates that increasing

the period can push the system to the symmetry-broken phase. The dashed gray line shows the location of the exceptional point. Equation 14 shows the advantage of diffraction gratings compared to Distributed Bragg Reflectors (DBRs) [30, 31]. This equation shows that in the diffraction gratings, in addition to real and imaginary parts of RI modulation, period and background refractive index can alter the system phase from symmetry to symmetry-broken phase. Thus, in a diffraction grating, more design freedom exists.

This section analytically solved the Helmholtz equation for the three first diffracted modes. We showed the impact of the imaginary part of RI modulation and period to shift the system from a PT-symmetry phase to the symmetry-broken stage. In the following section, we will design a grating and report the diffraction efficiency solved by the RCWA method. Moreover, the related electric field and amplitude distribution over the grating will be displayed, which gives us a depth understanding of physical mechanisms leading to extraordinary phenomena observed in PT-symmetric diffraction gratings.

III. NUMERICAL SIMULATIONS

Figure 4 displays a 3D schematic view of the designed diffraction grating, where yellow and red parts show the gain and loss, respectively. In this study, silicon dioxide was used as the substrate ($n_{sio_2} = 1.45$). The suggested material to design gain and loss parts is Lead-selenide (PbSe) as an active material with the real effective index of $n_{PbSe} = 5.07$.

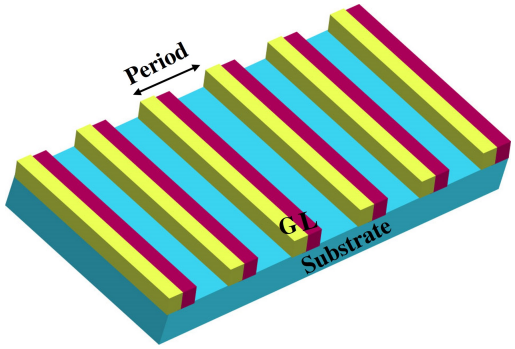

FIG. 4. 3D schismatic view of the PT-symmetric diffraction gratings.

One of the most well-known criteria of PT-symmetric systems is the spatial bifurcation of two modes in the symmetry-broken region. As presented in figure 2, in the symmetry-broken phase, two modes with the same frequency (same real part of eigenvalues) show the bifurcation, where one is captured mostly in the gain other trapped mainly in the loss. Thus, one mode is amplified while the other one is suppressed. This phenomenon is the primary mechanism behind the single-mode lasing in most of the PT-symmetric lasers. We expect that the numerical simulation demonstrates the same mechanism.

Figure 5 shows the spatial electric field distribution over a grating with the period of 1 μm and the thickness of 821 nm. Also, the substrate and gain/loss areas are demonstrated. Figure 5.(a) shows the symmetric distribution of the electric field over the gain and loss areas so that no mode experiences net amplification or suppression. This pattern can be associated with the PT-symmetry phase, where both eigenvalues are purely real. By increasing gain/loss (γ) from 0.2 to 0.21, the system is shifted to the symmetry-broken phase, where one mode is captured in the gain and experiences the amplification. Figure 5.(b) displays this mechanism clearly. However, the other mode is trapped in the loss and is suppressed (figure 5.c).

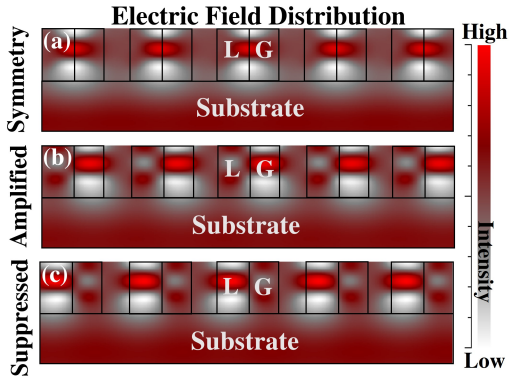

FIG. 5. Electric field distribution over the PT-symmetric grating where (a) $\gamma = 0.2$, associated with the symmetry phase .(b) $\gamma = 0.21$ associated with the symmetry-broken phase (amplified mode) .(c) $\gamma = 0.21$ associated with the symmetry-broken phase (suppressed mode).

After indicating the bifurcation over the PT-symmetric diffraction grating, we found out that the system can show a single-mode, almost zero-bandwidth (0.04 nm) lasing mode through optimizing gain/loss. Figure 6 shows the diffraction efficiency of the transmitted mode where the optimized value of γ equals 0.22. As this figure shows, over a broad spectrum range (1300 nm), the only lasing mode appeared at 1.46 μm. To better understand this non-trivial lasing mode, we compared the logarithm spectrum of the transmitted mode where $\gamma = 0.22$ and $\gamma = 0.21$. Figure 7 illustrates this comparison, where the solid red line is related to the system with $\gamma = 0.22$, and the dashed blue line is associated with $\gamma = 0.21$. Furthermore, the related amplitude distribution for each spectrum is shown over one period in the inset.

As figure 7 shows the diffraction efficiency of the transmitted mode when $\gamma = 0.22$ is 10^4 greater than when $\gamma = 0.21$. The primary reason for this huge difference can be related to the intensity of the confined field in the gain area. The inset illustrates that the amplitude of the confined mode in the gain area for the grating with $\gamma = 0.22$ is almost 10^2 greater than the amplitude of the

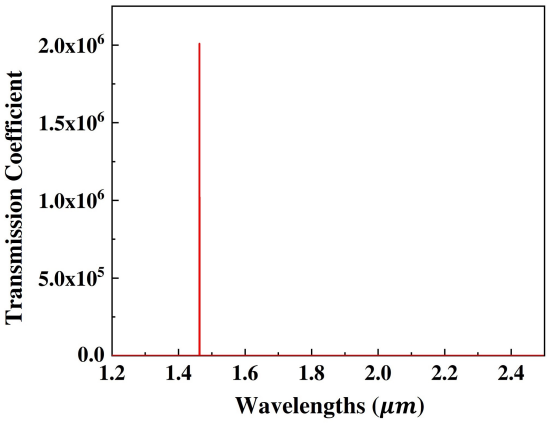

FIG. 6. The linear form of the transmitted spectrum over wavelengths from the grating with $\gamma = 0.22$.

trapped mode in the gain for the same grating but with $\gamma = 0.21$. The physical mechanism for this extraordinary phenomenon has roots in the scattering theory in PT-symmetric systems, and the concept of spectral singularity [32–34], which will be discussed in detail in the following paragraph.

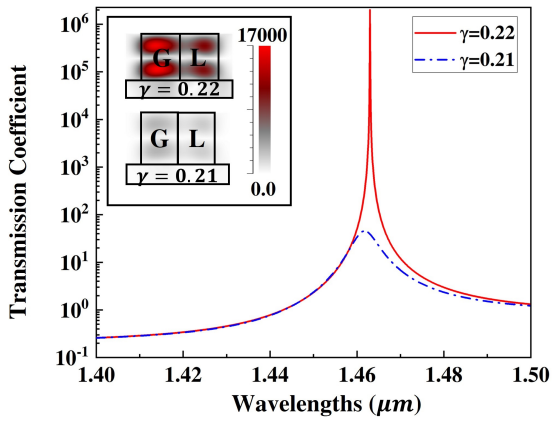

FIG. 7. The logarithm form of the transmitted spectra over wavelengths from the grating with $\gamma = 0.22$ (solid red line) and $\gamma = 0.21$ (dashed blue line). The amplitude distribution of each spectrum is displayed over one grating period in inset.

The properties of gratings as scattering systems can be defined by Scattering matrix (S-matrix). This matrix relates the input field to the output field, passing through a scattering system. Equation 15 shows the S-matrix (S_{nm}) that associates the incoming mode amplitude (ϕ_m) to the outgoing mode amplitude (η_n).

$$\sum_n S_{nm}(\omega)\phi_m = \eta_n \tag{15}$$

The required condition to define an S-matrix is the unitary condition (|det S|=1). For passive structures with real frequencies, this unitary condition is only satisfied by having unimodular S-matrix eigenvalues ($|s_\pm|=1$) [35]. Applying PT operator on S-matrix meets the unitary condition. However, in contrast with passive structures, in PT-symmetric systems, the only way to meet the unitary condition is not having unimodular eigenvalues. In these systems, the unitary condition can be satisfied by pairs reciprocal moduli as well ($s_\pm=1/s^*_\mp$) [36]. The former possibility to satisfy the unitary condition is related to the PT-symmetry (unimodular eigenvalues), and the latter way (reciprocal eigenvalues) is associated with the PT-symmetry-broken.

In the PT-symmetry-broken phase, there are points at which poles and zeros of the S-matrix intersect on the real axis [37, 38]. This intersection leads to approaching s_n to zero and consequently $1/s^*_n = \infty$, while their product is still unity. In fact, these singular points, named spectral singularity, correspond to the giant amplitude enhancement of diffracted modes for an optimized value of gain/loss.

SSs are a family member of resonant modes [39, 40]. However, the main feature for SSs that distinguishes them from trivial resonances is eliminating the imaginary part of the resonant frequencies [32]. The imaginary part of the resonant frequencies is responsible for evanescent energy or, in other words, the bandwidth of the resonant peaks, the lower evanescent energy, narrower bandwidth. The uniqueness of SSs lies in being purely real, which in theory leads to zero-bandwidth resonances [32]. It should be noted that SSs are different from the Bound States In Continuum (BICs); however, both show zero-bandwidth resonances [41].

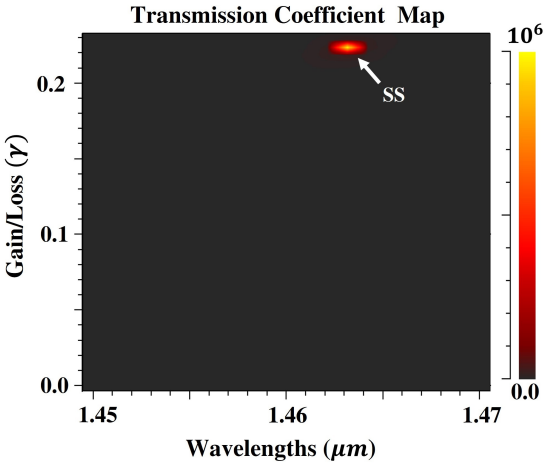

FIG. 8. The transmission coefficient map over wavelengths, where γ changes from 0 to 0.23. The colored bar shows the transmission coefficient value.

Figure 8 indicates the optimized value of gain/loss for the realization of SS in the designed grating. This figure shows the transmission coefficient map over wavelengths, where γ changes from 0 to 0.23. A considerable enhancement is observed at 1.463 μm when γ is 0.22. The point

marked with a white arrow shows that only at a specific gain/loss value, here ($\gamma = 0.22$), SS can occur, and higher or lower values cannot satisfy the SS condition. This is matched with the theory that claims only and only at the SS point, s_n goes to zero, while $1/s_n^*$ goes to ∞, and the giant transmission enhancement is related to $1/s_n^*$, which its amplitude approaches infinity. This transmission coefficient map indicates that by this unique diffraction grating design, $\gamma = 0.22$ leads to appearing one SS at 1.46 μm.

IV. CONCLUSION

In this study, for the first time, we investigated an active granting including gain and loss as an optical platform to realize the PT-symmetry concept. Herein, by solving the Helmholtz equation, the bifurcation leading to confining the amplified mode in the gain area was indicated. We showed that in diffraction gratings, in addition to gain/loss value, the period selection can move the system from PT-symmetry to the symmetry-broken phase. Moreover, a zero-bandwidth lasing mode at 1.463 μm was found through a numerical simulation. We suggest that this high Q-factor resonance mode can be the result of optimizing the gain/loss value, which locates the system in its spectral singularity, where one of the scattering states approaches zero while its reciprocal state approaches infinity. It should be noted that the method used for numerical simulation is the RCWA method. Considering the functionality of gratings in a broad range of applications, we anticipate introducing active PT-symmetric diffraction gratings can extend this range and offer new applications, including low-threshold and super-coherent lasers advancing the on-chip integrated optoelectronic devices.

[1] N. Bonod and J. Neauport, Diffraction gratings: from principles to applications in high-intensity lasers, Advances in Optics and Photonics **8**, 156 (2016).

[2] E. G. Loewen and E. Popov, *Diffraction gratings and applications* (CRC Press, 2018).

[3] D. Milner, K. Didona, and D. Bannon, High efficiency diffraction grating technologies lpdl 900 and lpdl 1100 in telecommunications applications, in *Optical Components and Materials II*, Vol. 5723 (International Society for Optics and Photonics, 2005) pp. 34–42.

[4] S. C. Barden, J. A. Arns, and W. S. Colburn, Volume-phase holographic gratings and their potential for astronomical applications, in *Optical Astronomical Instrumentation*, Vol. 3355 (International Society for Optics and Photonics, 1998) pp. 866–876.

[5] G. Ye, X. Li, and X. Wang, Diffraction grating of hydrogel functionalized with glucose oxidase for glucose detection, Chemical communications **46**, 3872 (2010).

[6] A. W. Wark, H. J. Lee, A. J. Qavi, and R. M. Corn, Nanoparticle-enhanced diffraction gratings for ultrasensitive surface plasmon biosensing, Analytical chemistry **79**, 6697 (2007).

[7] I. Nishi, T. Oguchi, and K. Kato, Broad-passband-width optical filter for multi/demultiplexer using a diffraction grating and a retroreflector prism, Electronics Letters **21**, 423 (1985).

[8] G. Almuneau, M. Condé, O. Gauthier-Lafaye, V. Bardinal, and C. Fontaine, High reflectivity monolithic sub-wavelength diffraction grating with gaas/alox stack, Journal of Optics **13**, 015505 (2010).

[9] C. Shi, X. F. Zang, L. Chen, Y. Peng, B. Cai, G. R. Nash, and Y. M. Zhu, Compact broadband terahertz perfect absorber based on multi-interference and diffraction effects, IEEE Transactions on Terahertz Science and Technology **6**, 40 (2015).

[10] I. Kaminow, H. Weber, and E. Chandross, Poly (methyl methacrylate) dye laser with internal diffraction grating resonator, Applied Physics Letters **18**, 497 (1971).

[11] L. Feng, Y. L. Xu, W. S. Fegadolli, M.-H. Lu, J. E. Oliveira, V. R. Almeida, Y.-F. Chen, and A. Scherer, Experimental demonstration of a unidirectional reflectionless parity-time metamaterial at optical frequencies, Nature materials **12**, 108 (2013).

[12] Y. Yang, H. Jia, Y. Bi, H. Zhao, and J. Yang, Experimental demonstration of an acoustic asymmetric diffraction grating based on passive parity-time-symmetric medium, Physical Review Applied **12**, 034040 (2019).

[13] C. M. Bender and S. Boettcher, Real spectra in non-Hermitian Hamiltonians having PT-symmetry, Physical Review Letters **80**, 5243 (1998).

[14] C. E. Rüter, K. G. Makris, R. ElGanainy, D. N. Christodoulides, M. Segev, and D. Kip, Observation of parity–time symmetry in optics, Nature physics **6**, 192 (2010).

[15] Ş. Özdemir, S. Rotter, F. Nori, and L. Yang, Parity-time symmetry and exceptional points in photonics, Nature materials **18**, 783 (2019).

[16] L. Feng, R. El-Ganainy, and L. Ge, non-Hermitian photonics based on parity–time symmetry, Nature Photonics **11**, 752 (2017).

[17] A. Guo, G. Salamo, D. Duchesne, R. Morandotti, M. Volatier-Ravat, V. Aimez, G. Siviloglou, and D. Christodoulides, Observation of p t-symmetry breaking in complex optical potentials, Physical review letters **103**, 093902 (2009).

[18] H. Ramezani, T. Kottos, R. El-Ganainy, and D. N. Christodoulides, Unidirectional nonlinear pt-symmetric optical structures, Physical Review A **82**, 043803 (2010).

[19] Z. Lin, H. Ramezani, T. Eichelkraut, T. Kottos, H. Cao, and D. N. Christodoulides, Unidirectional invisibility induced by PT–symmetric periodic structures, Physical Review Letters **106**, 213901 (2011).

[20] M. Kim, K. Kwon, J. Shim, Y. Jung, and K. Yu, Partially directional microdisk laser with two rayleigh scatterers, Optics letters **39**, 2423 (2014).

[21] X.-Y. Zhu, Y. L. Xu, Y. Zou, X.-C. Sun, C. He, M.-H. Lu, X.-P. Liu, and Y.-F. Chen, Asymmetric diffraction

based on a passive parity-time grating, Applied Physics Letters **109**, 111101 (2016).
[22] F. Gao, Y. M. Liu, X. D. Tian, C. L. Cui, and J. H. Wu, Intrinsic link of asymmetric reflection and diffraction in non-Hermitian gratings, Optics express **26**, 33818 (2018).
[23] T. K. Gaylord and M. Moharam, Analysis and applications of optical diffraction by gratings, Proceedings of the IEEE **73**, 894 (1985).
[24] T. Shui, W.-X. Yang, S. Liu, L. Li, and Z. Zhu, Asymmetric diffraction by atomic gratings with optical pt symmetry in the raman-nath regime, Physical Review A **97**, 033819 (2018).
[25] M. Berry and D. O'Dell, Diffraction by volume gratings with imaginary potentials, Journal of Physics A: Mathematical and General **31**, 2093 (1998).
[26] L. Dong, C. Huang, and W. Qi, Symmetry breaking and restoration of symmetric solitons in partially parity-time-symmetric potentials, Nonlinear Dynamics **98**, 1701 (2019).
[27] J. Yang, Symmetry breaking of solitons in one-dimensional parity-time-symmetric optical potentials, Optics letters **39**, 5547 (2014).
[28] B. Zhu, Q. J. Wang, and Y. D. Chong, Laser-mode bifurcations induced by pt-breaking exceptional points, Physical Review A **99**, 033829 (2019).
[29] L. Feng, Z. J. Wong, R. Ma, Y. Wang, and X. Zhang, Single-mode laser by parity-time symmetry breaking, Science **346**, 972 (2014).
[30] L. Feng, X. Zhu, S. Yang, H. Zhu, P. Zhang, X. Yin, Y. Wang, and X. Zhang, Demonstration of a large-scale optical exceptional point structure, Optics express **22**, 1760 (2014).
[31] Y. G. Boucher and P. Feron, Parity-time symmetry in laterally coupled bragg waveguides, IEEE Journal of Quantum Electronics **55**, 1 (2019).
[32] A. Mostafazadeh, Physics of spectral singularities, in *Geometric Methods in Physics* (Springer, 2015) pp. 145–165.
[33] L. Chaos-Cador and G. García-Calderón, Resonant states for complex potentials and spectral singularities, Physical Review A **87**, 042114 (2013).
[34] A. Mostafazadeh and H. Mehri-Dehnavi, Spectral singularities, biorthonormal systems and a two-parameter family of complex point interactions, Journal of Physics A: Mathematical and Theoretical **42**, 125303 (2009).
[35] C. Linton, Wave propagation. from electrons to photonic crystals and left-handed materials, by p. markoš and cm soukoulis: Scope: textbook. level: final year undergraduates and first year postgraduates (2009).
[36] Y. Chong, L. Ge, and A. D. Stone, Pt-symmetry breaking and laser-absorber modes in optical scattering systems, Physical Review Letters **106**, 093902 (2011).
[37] Y. Chong, L. Ge, H. Cao, and A. D. Stone, Coherent perfect absorbers: time-reversed lasers, Physical review letters **105**, 053901 (2010).
[38] D. G. Baranov, A. Krasnok, T. Shegai, A. Alù, and Y. Chong, Coherent perfect absorbers: linear control of light with light, Nature Reviews Materials **2**, 1 (2017).
[39] A. Mostafazadeh, Resonance phenomenon related to spectral singularities, complex barrier potential, and resonating waveguides, Physical Review A **80**, 032711 (2009).
[40] A. Mostafazadeh, Optical spectral singularities as threshold resonances, Physical Review A **83**, 045801 (2011).
[41] A. Mostafazadeh, Spectral singularities do not correspond to bound states in the continuum, arXiv preprint arXiv:1207.2278 (2012).